SHORT REPORT

ACG publications

Rec. Nat. Prod. 18:5 (2024) 526-531

records of natural products

Aspilactonol J: A New Cytotoxic Polyketide Isolated from the Marine-Derived Fungus *Aspergillus* sp. w2-13

Xiaomei Huang [1#], Shan Lin [3#], Guangyu Li [2], Zongze Shao [2], Weiyi Wang [*2] and Jinmei Xia [*2]

[1]*Applied Technology Engineering Center of Fujian Provincial Higher Education for Marine Resource Protection and Ecological Governance, Xiamen Key Laboratory of Intelligent Fishery, School of Marine Biology, Xiamen Ocean Vocational College, Xiamen 361100, P. R. China*
[2]*Key Laboratory of Marine Biogenetic Resources, Third Institute of Oceanography, Ministry of Natural Resources, Xiamen 361005, P. R. China*
[3]*Department of Orthopedics, the First Affiliated Hospital of Xiamen University, Xiamen 361003, P. R. China*

(Received June 11, 2024; Revised September 05, 2024; Accepted September 15, 2024)

Abstract: Marine-derived *Aspergillus* sp. strain w2-13, isolated from Dongshan Island in Fujian Province, produced five compounds through solid-state fermentation. This included a new polyketide, aspilactonol J (**1**), and four previously identified compounds (**2**–**5**). The structure of the new compound was determined using NMR, HR-MS, and ECD, supported by theoretical calculations. A plausible biosynthetic pathway for polyketides **1**–**3** was also proposed. Cytotoxicity tests on various cancer cell lines revealed that aspilactonol J (**1**) exhibited significant selectivity and efficacy, especially against HepG2 cells, suggesting its potential for pharmaceutical development. This study highlights the role of marine fungi as valuable sources of bioactive natural products with therapeutic potential.

Keywords: *Aspergillus*; polyketide; NMR; ECD; TDDFT; cytotoxic.

1. Microorganism Source

The strain w2-13 was isolated from a seawater sample collected near Dongshan Island, Fujian Province, China. Its ITS rDNA sequence has been submitted to the NCBI database (accession number: PP873196). A BLAST analysis revealed that the sequence of strain w2-13 exhibits a 100% similarity to that of *Aspergillus ochraceopetaliformis* strain MF4 (accession number: MH141440.1).

2. Previous Studies

Marine natural products often display unique structures and potent biological activities not found in their terrestrial counterparts, making them invaluable for novel drug discovery [1-3]. Fungi

* Corresponding author: E- Mail: wywang@tio.org.cn, xiajinmei@tio.org.cn
# These authors contribute equally to this article.

The article was published by ACG Publications
http://www.acgpubs.org/journal/records-of-natural-products September-October 2024 EISSN:1307-6167
DOI: http://doi.org/10.25135/rnp.477.2406.3552
Available online: September 30, 2024

from the genus *Aspergillus* are prolific sources of natural products. *Aspergillus* are widespread not only in terrestrial ecosystems but also in marine environments, where they have uniquely adapted to saline conditions [4, 5]. *Aspergillus* species are recognized for their ability to synthesize a diverse array of secondary metabolites, several of which exhibit notable biological properties [6-9]. Consequently, this genus has become a central focus in natural product research, yielding compounds with antitumor, antimicrobial, and anti-inflammatory properties [10]. Exploring *Aspergillus* species from marine sources thus offers a promising pathway for discovering novel natural products, highlighting the importance of these fungi in the search for new therapeutic agents [11].

3. Present Study

In this study, a new polyketide (**1**), along with two known polyketides (**2**–**3**) and two known sesquiterpenoid nitrobenzoyl esters (**4**–**5**) (Figure 1) were isolated from the marine-derived fungus *Aspergillus* sp. w2-13.

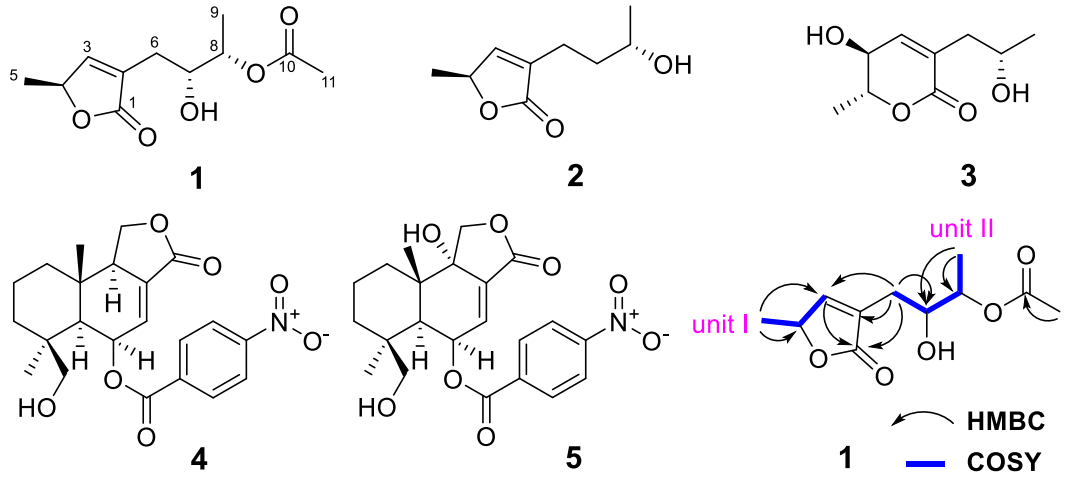

Figure 1. Chemical structures of compounds **1**–**5** and key COSY and HMBC correlations of **1**

Aspergillus sp. strain w2-13 was subjected to solid-state static fermentation using 150 1L Erlenmeyer flasks, each containing 70 g of rice, 30 g of millet, and 100 mL of seawater. After inoculation, the cultures underwent a 25-day incubation at 28°C. Subsequently, each flask underwent three rounds of extraction using 500 mL of ethyl acetate. The resulting extracts were concentrated under vacuo until dry, ultimately producing 117 g of crude extract. This crude extract was subjected to column chromatography on silica gel, eluting with a chloroform-methanol gradient (100:0 to 1:1). The eluent was fractionated into 70 separate 1 L portions. Based on thin-layer chromatography (TLC) analysis, similar components were combined as follows: fractions 1-13 into Group A, 14-21 into Group B, 22-34 into Group C, and 35-39 into Group D. Group B underwent decolorization using gel filtration chromatography (Sephadex LH-20, methanol). Subsequently, it was separated using reversed-phase silica gel column chromatography, employing a methanol-water gradient (100:0 to 0:100), followed by TLC to combine similar fractions, resulting in four subfractions (B1-B4). The B2 subfraction was further purified by medium-pressure liquid chromatography (MPLC) with a 10-50% acetonitrile-water gradient, yielding compound **3** (1.8 mg, t_R = 16.1 min). The B4 subfraction was separated using gel filtration chromatography (Sephadex LH-20, methanol), producing B4-1 and B4-2. B4-1 was further separated by MPLC using 50% acetonitrile in water, resulting in compound **5** (2.3 mg, t_R = 15.2 min). B4-2 was subjected to MPLC with 30% acetonitrile in water, resulting in the isolation of compound **4** (2.2 mg, t_R = 9.9 min). Group C was fractionated into C1-C6 using gel filtration chromatography (Sephadex LH-20, methanol). The C2 fraction was further subjected to separation using silica gel column chromatography with chloroform-methanol (10:1), producing two subfractions, C2-1 and C2-2. C2-2 was purified using MPLC with 45% acetonitrile in water, yielding compound **1** (2.5 mg, t_R = 19.3

min). C3 was decolorized using gel filtration (Sephadex LH-20, methanol) and then separated on a silica gel column with chloroform-methanol (15:1) as the eluent. Following TLC analysis, compound **2** (2.0 mg) was isolated.

*Aspilactonol J **(1)**:* A white amorphous powder; $[\alpha]_{25}^{D}$ +33.6 (*c* 0.05, MeOH); UV (MeOH) λ_{max} (log ε): 213 (3.83) nm; ECD (*c* 1 mg/mL, MeOH) λ_{max} ($\Delta\varepsilon$): 212 (4.18), 247 (-2.23) nm; HR-ESI-MS *m/z* 251.0901 $[M + Na]^+$ (calcd for $C_{11}H_{16}O_5Na$, 251.0895); IR (KBr) ν_{max} 3467, 2961, 2919, 2851, 1733, 1456, 1374, 1321, 1259, 1084, 1050, 1027, 955, 857, 801 cm^{-1} (Figure S10); ^1H and ^{13}C NMR data, Table 1.

Cytotoxic Assay: Cancer cell lines MCF7, HepG2, and L-02 were sourced from Wuhan Pricella Biotechnology Co., Ltd. (Wuhan, China). The cell lines were cultivated following established protocols. To assess the effects of compounds on cancer cell viability, CCK8 assays were conducted according to methods previously described [12].

NMR and ECD Calculations: The use of the CREST tool [13, 14] facilitated the generation of conformer candidates, and DFT calculations were executed employing the Gaussian 16 software. A comprehensive optimization and analysis of molecular conformers was performed, with details provided in the supplementary materials (Appendix S1).

NMR shielding constants were computed and converted to chemical shifts relative to TMS, and DP4+ probabilities were determined. Key statistical parameters such as R^2, the mean absolute error (MAE), and the corrected mean absolute error (CMAE) were also calculated. Detailed computational procedures and data are provided in Appendix S1.

Calculations using time-dependent density-functional theory (TDDFT) were performed with the CAM-B3LYP/6-311G(d) level in a methanol environment, utilizing the IEFPCM solvent model. For each conformer, 36 excited states were determined [15], and ECD spectra generation was carried out employing Multiwfn 3.6 software [16].

Table 1. ^1H (600 MHz) and ^{13}C (150 MHz) NMR data for compound **1** (in acetone-d_6, δ in ppm, *J* in Hz).

No.	Atom Type	δ_H (Multiplicity, *J*, nH)	δ_C
1	C	-	174.4
2	C	-	130.9
3	CH	7.42 (d, 1.5 Hz, 1H)	153.1
4	CH	5.07 (qd, 6.8,1.7 Hz, 1H)	78.4
5	CH_3	1.37 (d, 6.8 Hz, 3H)	19.3
6a	CH_2	2.47 (ddt, 15.1,3.6,1.7 Hz, 1H)	29.7
6b	CH_2	2.35 (ddt, 15.1,8.8,1.4 Hz, 1H)	29.7
7	CH	3.87 (m, 1H)	71.7
8	CH	4.78 (qd, 6.4,5.0 Hz, 1H)	73.7
9	CH_3	1.23 (d, 6.4 Hz, 3H)	15.5
10	C	-	170.5
11	CH_3	1.99 (s, 3H)	21.2

The molecular formula of **1** was determined to be $C_{11}H_{16}O_5$ based on the sodium adduct ion at *m/z* 251.0901 (Figure S8), indicating four degrees of unsaturation. Detailed spectroscopic studies, such as ^1H NMR, ^{13}C NMR, HSQC, and DEPT-135 analyses (Figures S1-S4), identified specific structural features that are detailed in Table 1 and Table S24. These included two ester carbonyls (δ_C 174.4, 170.5), one sp^3 methylene ($\delta_{C/H}$ 29.7/2.47 & 2.35), one olefinic sp^2 methine ($\delta_{C/H}$ 153.1/7.42), three oxygenated sp^3 methines ($\delta_{C/H}$ 78.4/5.07, 71.7/3.87, 73.7/4.78), one olefinic nonprotonated carbon (δ_C 130.9), and three methyl groups ($\delta_{C/H}$ 19.3/1.37, 15.5/1.23, 21.2/1.99). COSY correlation analysis (Figure S6) revealed two spin systems: C-3/C-4/C-5 (unit I) and C-6/C-7/C-8/C-9 (unit II). HMBC correlations of H_3-5 to C-3 and H-3 to C-1/C-2 (Figure S5), along with COSY correlations, confirmed the presence of an *α,β*-unsaturated *γ*-lactone moiety identified as 5-methylfuran-2(5*H*)-one in unit I.

HMBC correlations of H_2-6 to C-1/C-2/C-3 indicated that unit II was attached to C-2 (Figure 1). Chemical shifts ($\delta_{C/H}$ 71.7/3.87, 73.7/4.78) suggested that C-7 and C-8 were oxygenated. HMBC correlations of H8/H_3-11 to C-10 revealed that C-8 was linked to an acetoxy group. The derived structure comprised 11 carbons, 15 hydrogens, and 5 oxygens, confirming the presence of a hydroxy group attached to C-7.

The molecule featured three chiral carbons at C-4, C-7, and C-8. The absolute configuration at C-4 was assigned as *S* based on the positive π→π* Cotton effect at 210 nm and the negative n→π* Cotton effect at 240 nm. The coupling constant between H-7 and H-8 was 5.0 Hz, indicating an *erythro* configuration for the 7,8-diol. Two isomers, (4*S*,7*S*,8*R*)-**1** (**1a**) and (4*S*,7*R*,8*S*)-**1** (**1b**), were analyzed using NMR calculation at the mPW1PW91/6-31+G(d,p) level (Tables S1-S2). The isomer **1b** closely matched experimental data as indicated by parameters including R^2, MAE, and CMAE (Table S3), with a DP4+ probability of 86.98% (Figure S11, Table S3), excluding the possibility of **1a**. ECD calculations employing TDDFT at the CAM-B3LYP/6-311G(d) level (Tables S4-S23) corroborated these results, determining the absolute configuration of compound **1** to be 4*S*,7*R*,8*S*. (Figure 2, Figure S9).

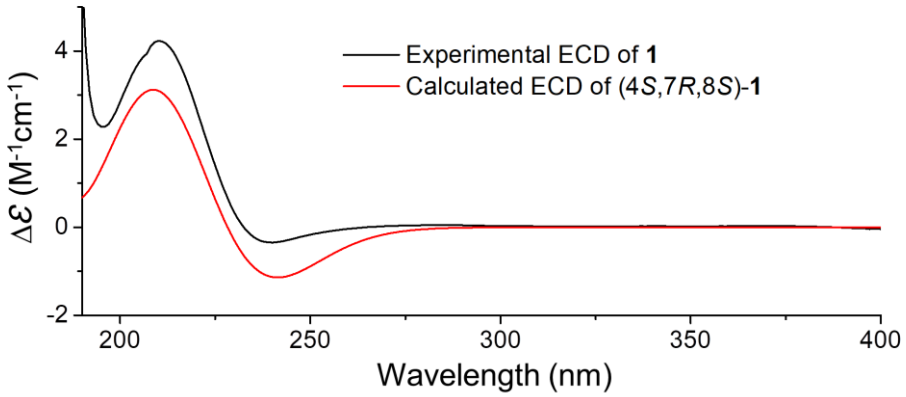

Figure 2. Experimental ECD curve of **1** and calculated ECD spectra of **1b** at CAM-B3LYP/6-311G(d)//B3LYP/6-31G(d)

Comparative analysis of NMR data with literature enabled the identification of the remaining four known compounds. These were aspilactonol (**2**) [17], dihydroaspyrone (**3**) [17], 14-hydroxy-6*β*-p-nitrobenzoylcinnamolide (**4**) [18] and 9*α*,14-hydroxy-6*β*-p-nitrobenzoylcinnamolide (**5**) [18].

The biosynthesis of compounds **1**, **2**, and **3** was initiated with the condensation of five C2 units via the polyketide synthase (PKS) pathway to form intermediate **a**. It was oxidized to generate **b**, which underwent molecular rearrangement to produce **c**. Further transformations of **c** through dehydration and decarboxylation led to **d**. Subsequent oxidation of **d** formed **e**, which underwent further oxidation to produce **f**. The transformations of **f** included lactonization to produce **h**, which upon reduction yielded compound **3**. Reduction and rearrangement of **f** formed **g**, and subsequent lactonization resulted in compound **2**. Meanwhile, reduction, hydration, and rearrangement of **f** produced **i**, which was converted into compound **1** through lactonization and acetylation (Figure 3).

At 20 μM, compound **1** selectively inhibited the three tested cancer cell lines, achieving a 63.88% inhibition rate in HepG2 cells. In contrast, the positive control drug, doxorubicin (Dox), demonstrated a non-selective inhibition rate exceeding 50% for all tested strains (Table 2). Compounds **2** and **3** displayed significantly lower inhibition rates, below 20% for all strains. IC_{50} values showed compound **1** at 17.1 μM and Dox at 73.0 nM on HepG2 cells (Figure S12). These findings indicate that compound **1** possesses a relatively moderate potency in inhibiting HepG2 cells.

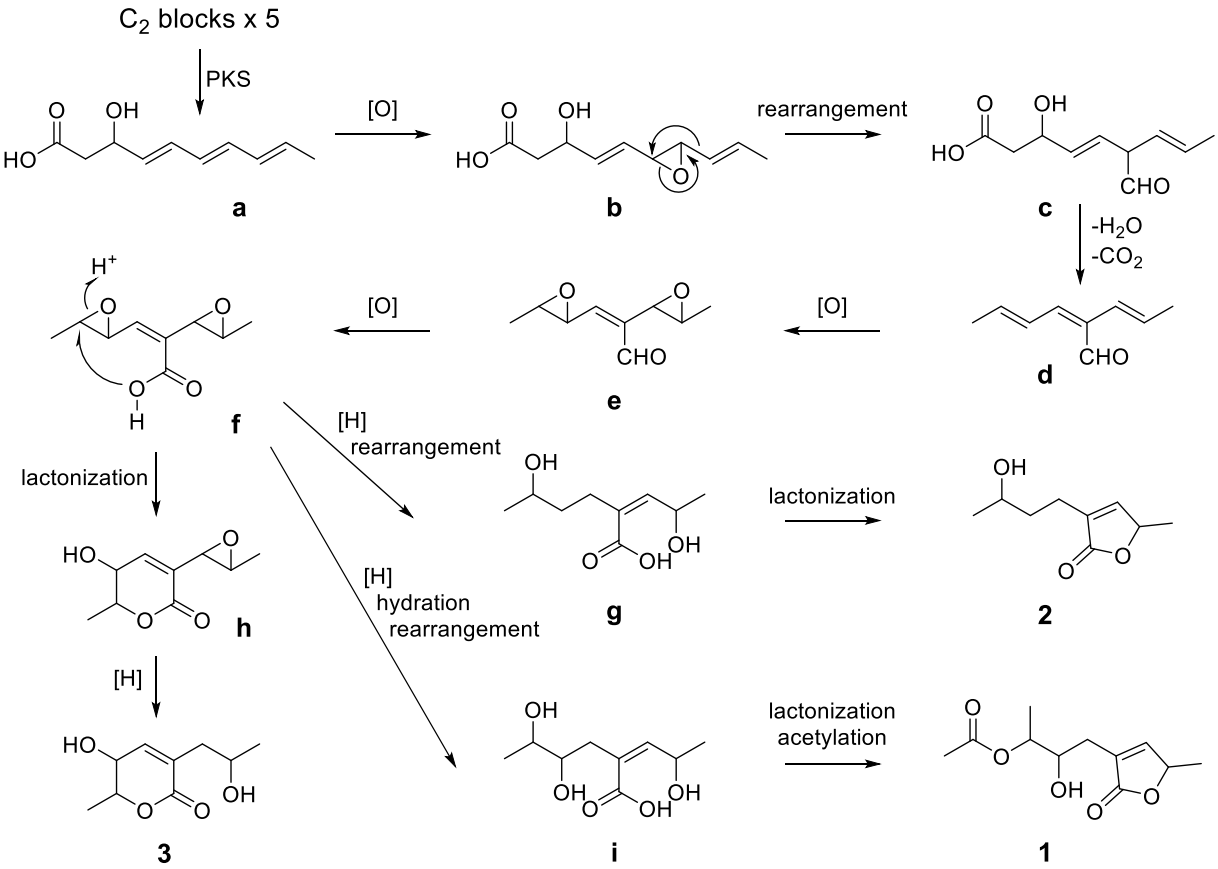

Figure 3. A plausible biosynthetic pathway for compounds **1**–**3**

Table 2. Inhibition rates of compounds **1**–**3** against three cancer cell lines

Compounds	Concentration (μM)	Cell inhibition rates ± SD (%)		
		MCF-7	HepG2	L-02
1	20	-2.46 ± 2.86 %	63.88 ± 3.81 %	1.21 ± 6.31 %
2	20	0.42 ± 2.90 %	1.95 ± 4.64 %	-0.92 ± 1.84 %
3	20	18.37 ± 2.01 %	4.63 ± 4.32 %	2.82 ± 1.67 %
Dox	10	51.48 ± 0.53 %	67.92 ± 1.38 %	98.42 ± 0.30 %

Acknowledgments

This work was supported by the National Key Research and Development Program of China (2022YFC2804100), the Scientific Research Foundation of Third Institute of Oceanography, MNR (2022007), Xiamen Southern Oceanographic Center Project (22GYY007HJ07), Natural Science Foundation of Fujian Province (2021J01509), the COMRA Program (DY135-B2-01), Research Projects for High-level Talents of Xiamen Ocean Vocational College (140008), and Open Funding Project of Key Laboratory of Marine Biogenetic Resources, Third Institute of Oceanography, Ministry of Natural Resources (HY202303 & HY202307).

Supporting Information

Supporting Information accompanies this paper on http://www.acgpubs.org/journal/records-of-natural-products

ORCID
Weiyi Wang: 0000-0003-3163-9491
Jinmei Xia: 0000-0001-9499-5560
Xiaomei Huang: 0009-0004-3542-9138
Shan Lin: 0009-0001-0110-9361
Guangyu Li: 0000-0001-8807-1425
Zongze Shao: 0000-0002-4784-090X

References

[1] A. R. Carroll, B. R. Copp, T. Grkovic, R. A. Keyzers and M. R. Prinsep (2024). Marine natural products, *Nat. Prod. Rep.* **41**, 162-207.
[2] A. R. Carroll, B. R. Copp, R. A. Davis, R. A. Keyzers and M. R. Prinsep (2023). Marine natural products, *Nat. Prod. Rep.* **40**, 275-325.
[3] A. R. Carroll, B. R. Copp, R. A. Davis, R. A. Keyzers and M. R. Prinsep (2022). Marine natural products, *Nat. Prod. Rep.* **39**, 1122-1171.
[4] H. Jangid, S. Garg, P. Kashyap, A. Karnwal, A. Shidiki and G. Kumar (2024). Bioprospecting of *Aspergillus* sp. as a promising repository for anti-cancer agents: a comprehensive bibliometric investigation, *Front. Microbiol.* **15**, 1379602.
[5] S. Agrawal, P. Chavan and L. Dufosse (2024). Hidden treasure: halophilic fungi as a repository of bioactive lead compounds, *J. Fungi (Basel)* **10**,
[6] W. Zhao, J. Yi, Y. Chang, C. Sun and X. Ma (2022). Recent studies on terpenoids in *Aspergillus* fungi: chemical diversity, biosynthesis, and bioactivity, *Phytochemistry* **193**, 113011.
[7] G. Currens, U. Sankpal, R. Basha and E. Cheng (2022). Cytotoxic activities of Aspergillin PZ and Trichoderone B from an ısolate of *Aspergillus flavipes* sp. against NCI-60 human tumor cell lines, *Rec. Nat. Prod*.**16**, 104-109.
[8] Y. Jiang, C. Jiang, Q. Zhou, Y. Tong and P. Wang (2022). A new alkaloid from the endophytic fungus of *Crocus sativus* L., *Aspergillus fumigatus* Y0107, *Rec. Nat. Prod*.**16**, 463-470.
[9] L. Xu, G. Liu, Y. Chen, S. Liu, W. Luo , P. Hu , C. Huang , X. Ji , S. Wan and G. Cao (2022). Cytotoxic drimane-type sesquiterpenoids from the fungus *Aspergillus flavipes* 297, R*ec. Nat. Prod*.**16**, 488-492.
[10] H. E. Elsayed, R. A. Kamel, R. R. Ibrahim, A. S. Abdel-Razek, M. A. Shaaban, M. Frese, N. Sewald, H. Y. Ebrahim and F. A. Moharram (2021). Cytotoxicity, antimicrobial, and *in silico* studies of secondary metabolites from *Aspergillus* sp. isolated from *Tecoma stans* (L.) Juss. ex Kunth leaves, *Front. Chem.* **9**, 760083.
[11] A. Hagag, M. F. Abdelwahab, A. M. Abd El-Kader and M. A. Fouad (2022). The endophytic *Aspergillus* strains: a bountiful source of natural products, *J. Appl. Microbiol.* **132**, 4150-4169.
[12] W. Wang, J. W. Cheng, J. J. Qin, B. Hu, X. Li, B. Nijampatnam, S. E. Velu, J. Fan, X. R. Yang and R. Zhang (2019). MDM2-NFAT1 dual inhibitor, MA242: Effective against hepatocellular carcinoma, independent of p53, *Cancer Lett.* **459**, 156-167.
[13] P. Pracht, F. Bohle and S. Grimme (2020). Automated exploration of the low-energy chemical space with fast quantum chemical methods, *Phys. Chem. Chem. Phys.* **22**, 7169-7192.
[14] S. Grimme (2019). Exploration of chemical compound, conformer, and reaction space with meta-dynamics simulations based on tight-binding quantum chemical calculations, *J. Chem. Theory Comput.* **15**, 2847-2862.
[15] G. Pescitelli and T. Bruhn (2016). Good computational practice in the assignment of absolute configurations by TDDFT calculations of ECD spectra, *Chirality* **28**, 466-474.
[16] T. Lu and F. Chen (2012). Multiwfn: a multifunctional wavefunction analyzer, *J. Comput. Chem.* **33**, 580-592.
[17] X. W. Chen, C. W. Li, C. B. Cui, W. Hua, T. J. Zhu and Q. Q. Gu (2014). Nine new and five known polyketides derived from a deep sea-sourced *Aspergillus* sp. 16-02-1, *Mar. Drugs* **12**, 3116-3137.
[18] G. N. Belofsky, P. R. Jensen, M. K. Renner and W. Fenical (1998). New cytotoxic sesquiterpenoid nitrobenzoyl esters from a marine isolate of the fungus *Aspergillus versicolor*, *Tetrahedron* **54**, 1715-1724.